



**Hybridization-specific chemical reactions to create
interstrand crosslinking and threaded structures of nucleic
acids**

Journal:	<i>Organic & Biomolecular Chemistry</i>
Manuscript ID	OB-REV-03-2022-000551.R1
Article Type:	Review Article
Date Submitted by the Author:	18-May-2022
Complete List of Authors:	Onizuka, Kazumitsu; Tohoku University Yamano, Yuuhei; Tohoku University Abdelhady, Ahmed ; Tohoku University Nagatsugi, Fumi; Tohoku University,

REVIEW

Hybridization-specific chemical reactions to create interstrand crosslinking and threaded structures of nucleic acids

Received 00th January 20xx,
Accepted 00th January 20xx

Kazumitsu Onizuka,^{*a,b,c} Yuuhei Yamano,^{a,b} Ahmed Mostafa Abdelhady,^{a,b,d} and Fumi Nagatsugi^{*a,b}

DOI: 10.1039/x0xx00000x

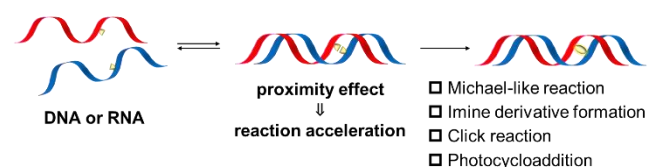
The interstrand crosslinking and threaded structures of nucleic acids have high potential in oligonucleotide therapeutics, chemical biology, and nanotechnology. For example, properly designed crosslinking structures provide high activity and nuclease resistance for anti-miRNAs. The noncovalent labeling and modification by the threaded structures are useful as new chemical biology tools. Photoreversible crosslinking creates smart materials, such as reversible photoresponsive gels and DNA origami objects. This review introduces the creation of interstrand crosslinking and threaded structures, such as catenanes and rotaxanes, based on hybridization-specific chemical reactions and their functions and perspectives.

1. Introduction

The formation of a duplex structure of nucleic acids can accelerate various specific chemical reactions through proximity effect between the reaction points because reactive groups can be rationally placed at specific positions (Figure 1). This is often referred to as a templated reaction. Using these hybridization-specific chemical reactions skillfully, various crosslinking and threaded structures, such as catenanes and rotaxanes, can be created. The created nucleic acids often have a unique structure and high potential in oligonucleotide therapeutics, chemical biology, and nanotechnology. For example, the properly designed crosslinking structures provide high activity and nuclease resistance for anti-miRNAs. The noncovalent labeling and modification by the threaded structures are useful as new chemical biology tools. Photoreversible crosslinking creates smart materials, such as reversible photoresponsive gel and DNA origami objects. Thus, various reactions have been developed and investigated to create structures with new functions.

Several hybridization-based templated reactions and their reviews have been reported.¹⁻⁵ In the templated reactions, two types of reactions, interstrand crosslinking and strand ligation, are often used to create functional structures. For the interstrand crosslinking, various reactions based on Michael-like reactions, imine derivative formation, click reaction, and photocycloaddition have been used (Figure 1A).

A. Interstrand crosslinking



B. Strand ligation

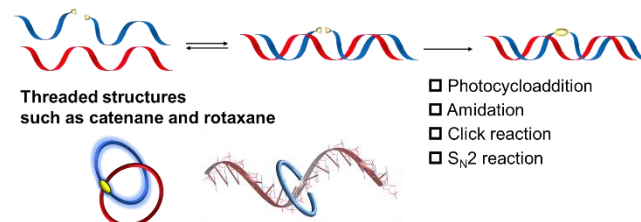


Figure 1. Illustration and example of hybridization-specific chemical reactions. (A) Interstrand crosslinking. (B) Strand ligation.

reaction, and photocycloaddition have been used (Figure 1A). In addition, for creating threaded structures, such as catenanes and rotaxanes, strand ligation-type templated reactions, such as photocycloaddition, amidation, click reaction, and S_N2 reactions, have been used (Figure 1B). This review paper introduces hybridization-specific chemical reactions to create interstrand crosslinking and threaded structures of nucleic acids and discusses their functions and perspectives.

2. Creation of interstrand crosslinking structures

We have developed the crosslinking reactions using vinyl chemistry for many years (Figure 2).⁶⁻¹⁹ We initially developed a 2-amino-6-vinylpurine (AVP) base as a covalent warhead

^a Institute of Multidisciplinary Research for Advanced Materials, Tohoku University, 2-1-1 Katahira, Aoba-ku, Sendai, Miyagi 980-8577, Japan.

E-mail: onizuka@tohoku.ac.jp

E-mail: nagatsugi@tohoku.ac.jp

^b Department of Chemistry, Graduate School of Science, Tohoku University, Aoba-ku, Sendai 980-8578, Japan.

^c Division for the Establishment of Frontier Sciences of Organization for Advanced Studies, Tohoku University, Aoba-ku, Sendai, Miyagi 980-8577, Japan.

^d Department of Chemistry, Faculty of Science, Al-Azhar University, Nasr City, 11884, Cairo, Egypt.

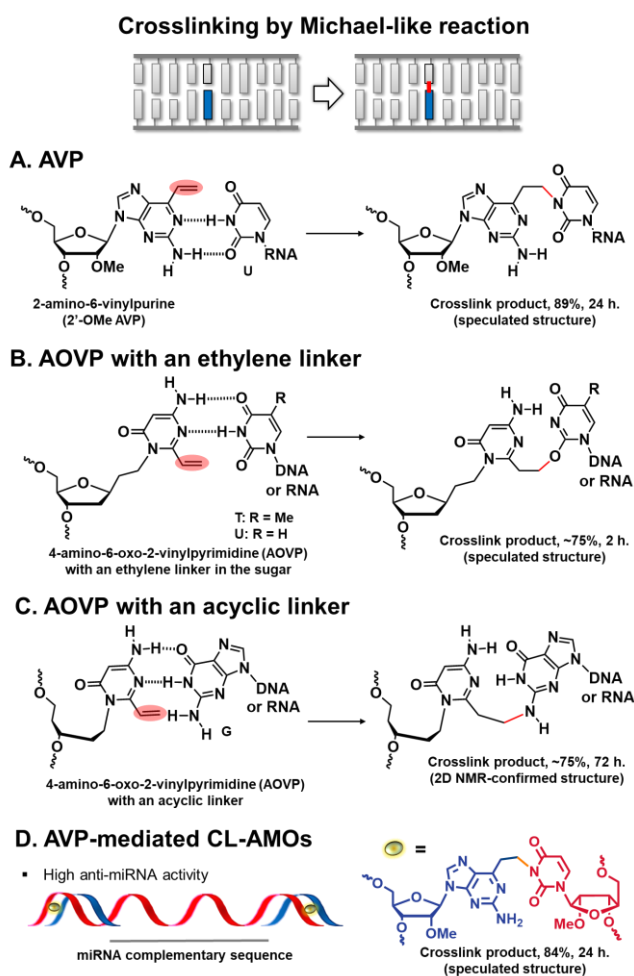


Figure 2. Interstrand crosslinking reactions by the Michael-like reaction. The reactions using (A) AVP,^{6-8,28} (B) AOVP with an ethylene linker,¹⁰ and (C) AOVP with an acyclic linker.¹⁵ (D) AVP-mediated CL-AMOs.²⁸

(Figure 2A).⁶⁻⁹ The AVP base has a reactive vinyl group and reacts with thymidine (T) and uridine (U) bases in the complementary positions of DNA and RNA, respectively, under neutral conditions (Figure 2A). In the duplex between AVP-containing RNA and 2'-OMe RNA, the vinyl group can approach the N3 atom of the U base, and Michael-type reaction efficiently proceeds. These efficient reactions were not observed at the monomer level, suggesting that the proximity effect is significant for the vinyl reaction. Additionally, vinyl reactivity and selectivity can be modulated by changing the base and sugar structure of the vinyl compound.¹⁰⁻¹⁹ For example, 4-amino-6-oxo-2-vinylpyrimidine (AOVP) with an ethylene linker in the sugar component selectively reacts at the complementary sites of T and U bases in DNA and RNA, respectively (Figure 2B). Conversely, AOVP with an acyclic linker produces adducts with the G and T bases in DNA and G base in RNA (Figure 2C).¹⁵ These results suggest

Y. Komatsu *et al.* (2012, 2018)

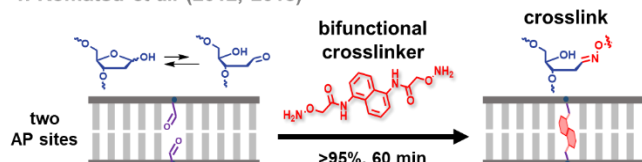


Figure 3. Interstrand crosslinking through oxime formation using two AP sites.^{29,30}

that selective crosslinking reactions can be achieved by the proper arrangement of vinyl groups, even with pyrimidine derivatives. This vinyl chemistry can also be applied to develop reactive small molecules, and we have reported several compounds.²⁰⁻²⁶ The vinyl derivative-containing oligonucleotides were developed to control gene expression by crosslinking formation. For creating a functional crosslinking structure, we used vinyl chemistry to synthesize crosslinked RNA²⁷ and 2'-OMe RNA duplexes.²⁸ This vinyl crosslinking kept a native structure and provided high thermal stability. The native-like crosslinking structure is advantageous for the biochemical study and development of nucleic acid-based medicines because the introduction of large artificial moiety often decreases enzyme binding affinity. In the study of the native-like crosslinked-RNA duplex, the crosslinked-RNA duplex had a slightly higher binding affinity with adenosine deaminase acting on RNA type 2 (ADAR2) than the native RNA.²⁷ In the study of the crosslinked 2'-OMe RNA duplexes, we synthesized anti-miRNA oligonucleotides (AMOs) with a flanking crosslinked-duplex structure using AVP (Figure 2D). These crosslinked AMOs containing the antisense-targeting miR-21 showed a markedly higher anti-miRNA activity than the commercially available miR-21 inhibitor, which has locked nucleic acid residues.²⁸

Prior to the research on AVP-crosslinking AMOs, Komatsu *et al.* reported AMOs with flanking crosslinked-duplex structures, which were prepared using a short bifunctional crosslinker containing bis-aminoxy groups and a pair of apurinic/aprimidinic (AP) sites (Figure 3).^{29,30} The bifunctional linker intercalated in the AP sites and efficiently formed crosslinked-duplex DNA and 2'-OMe RNA via the oxime formation reaction between oxyamine and the aldehyde of an AP site. Compared with other structured AMOs, the AMO flanking crosslinked-duplex structures at the 5' and 3' terminals exhibited a higher inhibitory activity in cells. The 3'-side crosslinking improved nuclease resistance, whereas the 5'-side crosslinking contributed to binding with miRNA in Argonaute (Ago). These structure–function relationship analyzes of AMOs provide essential insights into the function control of Ago–miRNA complexes. In addition, the crosslinked AMOs did not induce an immune response and showed no significant cytotoxicity in cells. Thus, further structure–function relationship analysis of the crosslinked AMOs and detailed investigation of the inhibition mechanism are required.

Using an AP site, Gates et al. reported another type of interstrand crosslinking reaction (Figure 4).³¹⁻³⁶ In this reaction, the aldehyde group of the AP site reacts with the exocyclic amino group of the purine base in the opposite strand of the duplex to provide an imine-derived linkage (Figure 4A).³¹⁻³⁵ The crosslinking occurred more efficiently when

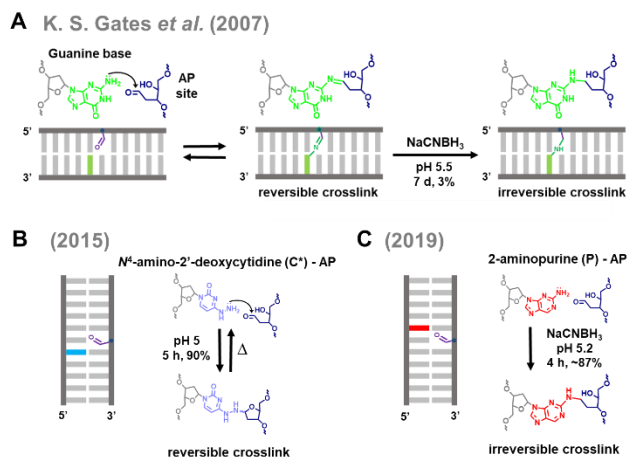


Figure 4. Interstrand crosslinking by imine derivative formation using an AP site. The reaction between the AP site and (A) guanine base³¹, (B) N^4 -amino-2'-deoxycytidine³⁴, or (C) 2-aminopurine³⁵ in the opposite strand.

N^4 -amino-2'-deoxycytidine (C*)³⁴ and 2-aminopurine (P)³⁵ were used instead of the canonical purine bases (Figures 4B and C). Although these crosslinking products were reversible, reductive amination with sodium cyanoborohydride enabled irreversible crosslinking. Moreover, the optimum arrangement of the AP site and nucleobase differs for each nucleobase. For example, the 5'-AP A/3'-A C* sequence is suitable for the C*-AP crosslinking (Figure 4B), whereas a differently arranged 5'-T AP/3'-P A sequence is appropriate for the P-AP crosslinking (Figure 4C). These reports not only provide insights into various lesions that can occur via the AP sites, but also suggest that these crosslinks are promising for creating interstrand crosslinking structures with minimal artificial modifications.

The click reaction, particularly copper-catalyzed azide-alkyne cycloaddition (CuAAC), is a powerful reaction. Many papers have reported nucleic acid conjugation and crosslinking via these reactions.³⁷⁻⁴² As an example of crosslinking reactions, rapid and efficient DNA crosslinking was achieved using two oligo DNAs (ODNs) containing 5-octadiynyl dU and 5-azido-modified dU (Figure 5A).⁴³ For creating a functional structure, dumbbell-shaped clicked ODNs were synthesized using ODN containing *N*-3-(azidoethyl)thymidine and *N*-3-(propargyl)thymidine at the 3'- and 5' terminals (Figure 5B).⁴⁴ The dumbbell-shaped ODNs were thermally and enzymatically stable and had the ability to bind to NF- κ B p50 homodimers within a similar range to that of a control double-stranded decoy ODN. As shown by both examples, the high reaction yield and relatively high flexibility of the reaction distance are the advantages of CuAAC crosslinking.

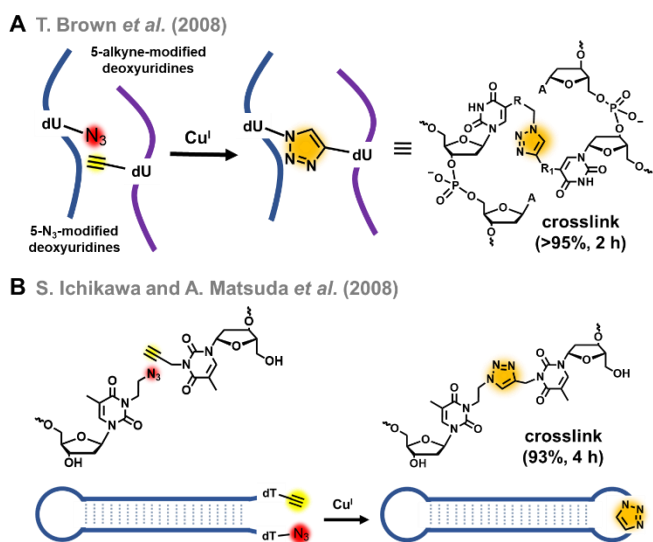


Figure 5. Crosslinking by CuAAC. The reaction creates (A) the crosslinking duplex⁴³ and (B) the dumbbell-shaped ODN.⁴⁴

Photocycloaddition is often used for crosslinking. Fujimoto et al. developed many crosslinkers toward pyrimidine bases. The 3-cyanovinylcarbazole (^{CNV}K) base is one of the most potent photo-crosslinkers for crosslinking the vinyl component of the ^{CNV}K base and double bond of pyrimidine bases.⁴⁵ This [2 + 2] photocycloaddition reaction proceeded after only 1 s by photoirradiation at 366 nm (Figure 6A). Furthermore, the reverse reaction occurred for 60 s by photoirradiation at 312 nm. Recently, the reaction rate⁴⁶ was further improved and the wavelength of the forward and reverse reactions⁴⁷ was lengthened by changing the vinylcarbazole base structure. This type of crosslinking has been used for many applications, such as the inhibition of translation^{48, 49}, RNA editing^{50, 51}, RNA fluorescence in situ hybridization⁵²⁻⁵⁴, functional gel material engineering⁵⁵, and DNA origami⁵⁶. In DNA nanotechnology, the photoreversible crosslinking property of ^{CNV}K is one of the advantages of creating smart materials. For example, photoresponsive DNA gels, which undergo repetitive sol-gel transitions in response to different photoirradiation wavelengths and temperatures, were developed using the property of ^{CNV}K in a suitable position at the sticky ends of the X-shaped DNA structure (Figure 6B).⁵⁵ This technique could have potential applications in medicine (e.g., drug delivery). Despite the formation of a stable DNA origami under different cation concentrations is challenging, ^{CNV}K can offer a photochemical strategy for forming reversible covalent bonds across the stacking contacts of DNA origami (Figure 6C).⁵⁶ A coumarin analog can also be used for establishing reversible interstrand crosslinking to pyrimidine bases.⁵⁷

As another example of reversible crosslinking, Asanuma et al. developed photocrosslinkers based on stilbene derivatives tethered with a D -threoninol linker.^{58, 59} The photocycloaddition reaction between two overlapping styrylpyrene moieties on DNA duplex was triggered by 455-nm visible-light irradiation (Figure 7A). The reverse reaction was

realized with 340-nm UV-light irradiation. Using a similar photoreaction for intrastrand linkage, the photocontrol of serinol nucleic acid (SNA)/RNA duplex formation was also achieved (Figure 7B).^{60, 61} As an application of this type of photocrosslinking, terminally photocrosslinked siRNAs with stilbene derivatives were prepared. They showed high

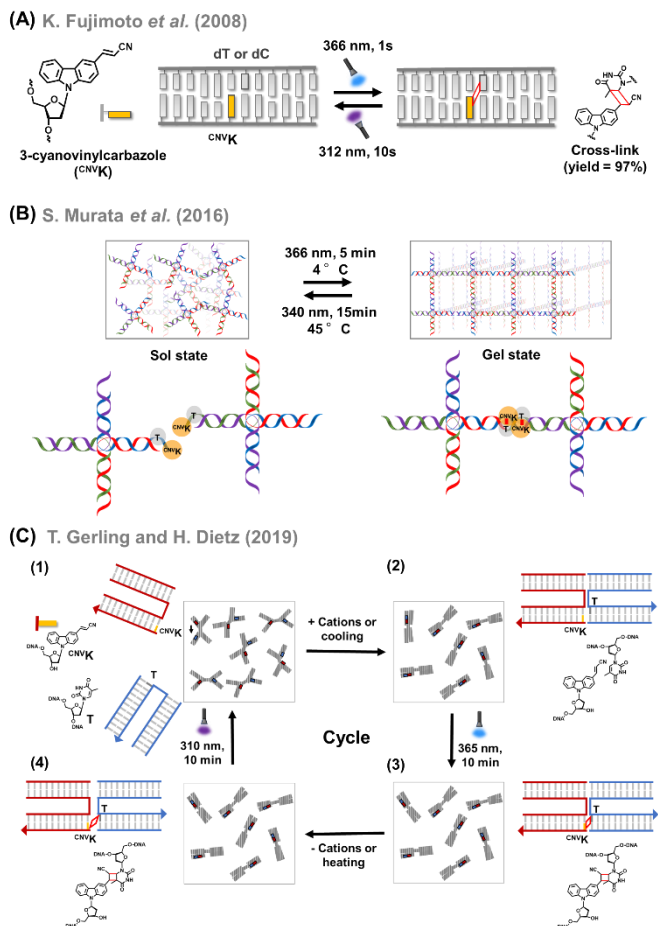


Figure 6. Reversible interstrand photocrosslinking using 3-cyanovinylcarbazole (CNVK).⁴⁵ (A) Upon 366-nm light irradiation, CNVK undergoes a [2 + 2] cycloaddition reaction with the pyrimidine base in the complementary strand. Cycloreversion proceeds with 312-nm light irradiation. (B) Gel-sol transition of X-motif with CNVK .⁵⁵ Transitions are triggered by photocrosslinking and cleaving. (C) Schematic of the photocrosslinking and photocleavage of CNVK -modified nucleosides across stacking contacts for the DNA origami switch object.⁵⁶

nuclease resistance while retaining the RNAi activity (Figure 7C).⁶² The crosslinking reaction was also used in the DNA-encoded dynamic library.⁶³ This crosslinking method that can additionally introduce photocrosslink type molecules via acyclic linkers has the advantage of creating strong linkages with only a slight disturbance of the nucleic acid structure.

The DNA crosslinking by the [2 + 2] photocycloaddition reaction was achieved using flipping-out-induced ODNs (Figure 8).⁶⁴ We developed several flipping-out-induced bases based on the original alkylated-thymidine structure.²² Alkene-type

flipping-out-induced bases (Ph(alkene) and An(alkene)) are 5-methylpyridone derivatives linked to an aromatic compound with an alkene linker at the C3 position.⁶⁴ In particular, Ph(alkene) efficiently provided the crosslinked product in high yield after only 10 s of photoirradiation when the alkenes in the duplex DNA overlapped. The photoirradiation induced isomerization to produce crosslinked isomers (Figure 8). This highly efficient reaction provided a crosslinked product, even when a duplex with a low T_m value was used.

In addition, we developed alkyne-type flipping-out-induced bases (Ph(alkyne) and An(alkyne)) with an alkyne linker instead of an alkene linker at the C3 position (Figure 9).⁶⁵ In this case, efficient alkyne-alkyne photocrosslinking was realized using the heterocombination of Ph(alkyne) and An(alkyne) rather than a homocombination, such as Ph-Ph and An-An. The difference in the reaction rates between the hetero and homocombinations occurred because single electron transfer (SET) is essential for alkyne-type reactions, i.e., SET occurs more readily for the heterocombinations than for the homocombinations because of the difference in redox potential. In our postulated photoreaction mechanism based on several reports on the photoinduced [2 + 2 + 2] cycloaddition reactions (Figure 9)⁶⁶⁻⁶⁸, the first step is affected

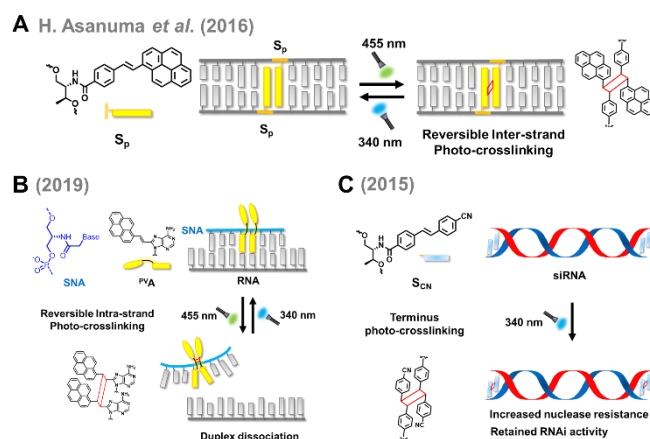


Figure 7. Reversible photocrosslinking using stilbene derivatives tethered with an acyclic linker. (A) Reversible interstrand photocrosslinking using styrylpyrene (S_p).⁵⁹ (B) Photocontrol of the duplex formation between serinol nucleic acid (SNA) and RNA using photocrosslinkable nucleobase 8-pyrenylvinyl adenine (PVA).⁶⁰ (C) Preparation of terminus crosslinked siRNA using photocrosslinking of *p*-cyanostilbene (S_{CN}).⁶²

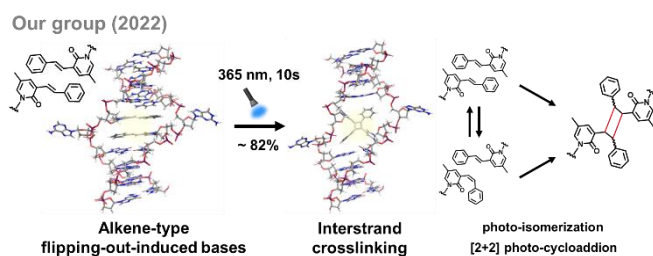


Figure 8. Interstrand photocrosslinking using alkene-type flipping-out-induced bases.⁶⁴ Photoirradiation at 365-nm mediates the photoisomerization of the flip-out-induced bases. Both isomers can form crosslinking via [2 + 2] photocycloaddition.

by the base combinations. One Ar base is excited, and SET occurs between the excited and unexcited Ar bases to give the

Our group (2019)

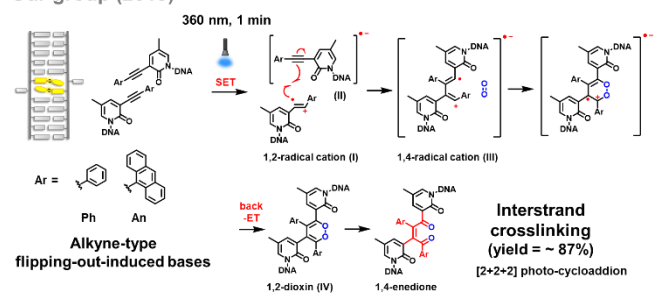


Figure 9. Postulated reaction mechanism of alkyne-alkyne photocrosslinking on the flipping-out and base-stacked field.⁶⁵

1,2-radical cation (I) and the reduced radical anion base (II) on the flipping-out and base-stacked field. The radical anion may delocalize on the DNA duplex. The 1,2-radical cation (I) reacts with the alkyne (II) to provide the 1,4-radical cation (III). The following cyclization with O₂ and the back electron transfer (back-ET) provide a neutral 1,2-dioxin (IV). After O–O bond cleavage, a 1,4-enedione crosslinked product is generated. Because these crosslinks provide a unique flipped-out structure, exploring the novel biological functions including the above anti-miRNA activity would be interesting. In nanotechnology applications, the flipped-out bases may be used as additional interaction and modification scaffolds to create new materials.

3. Creation of threaded structures

In nucleic acid chemistry, threaded and interlocked molecular architectures, such as catenanes and rotaxanes, have been studied for DNA nanotechnology,^{69–80} topological labels,^{81, 82} and complexes' stabilization.^{83, 84} Generally, these are constructed enzymatically using a ligase. Alternatively, various chemical methods have been developed to construct such architectures and expand their application. In particular, template-assisted chemical strand ligation can realize an enzyme-like construction.

Similar to crosslinking, the [2 + 2] photocyclization reaction is a powerful method for creating threaded and interlocked structures. For example, 5-vinyl-2'-deoxycytidine (^VC) and 5-carboxyvinyl-2'-deoxyuridine (^{CV}U) were used to create catenanes toward single- and double-stranded circular DNA, respectively.^{85, 86} As shown in Figure 10, the ^{CV}U base-containing probe ODN formed a triple helix with the plasmid. Upon irradiating with 366 nm light for 1–3 h, the probe ODN was cyclized by the [2 + 2] cycloaddition reaction between the 5' and 3' terminals of the ^{CV}U and C bases of the probe ODN.⁸⁶ The formation of a helical triplex structure is important to ensure that the probe ODN penetrates the plasmid ring to form the threaded structures. A more efficient catenane formation may be achieved using a probe that forms

a more stable triplex or by adopting the photoreactive bases with a high ligation efficiency. The reverse reaction with

K. Fujimoto and I. Saito *et al.* (2007)

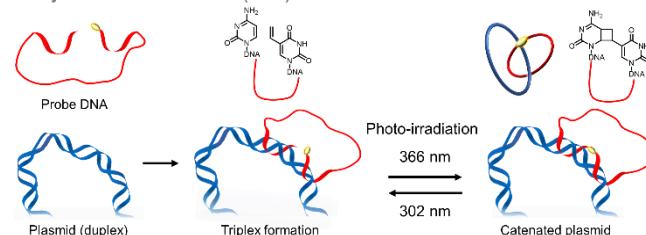
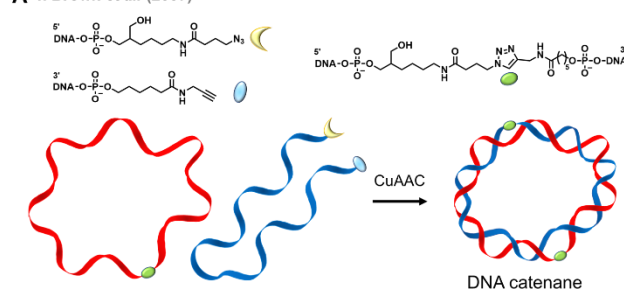


Figure 10. Catenane formation via the [2 + 2] photocyclization reaction.⁸⁶ The probe DNA, which forms triplex with plasmid DNA, cyclizes upon 340-nm irradiation to form the catenated plasmid. This interlocked structure can be unlocked using 302-nm irradiation.

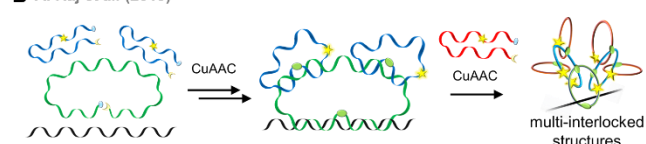
302-nm photoirradiation for 1 h almost entirely unlocked this catenated plasmid. The reversible photo [4 + 4] cycloaddition of anthracene is a useful reaction for the strand ligation and photocyclization.^{87, 88}

CuAAC is often used for chemical ligation as well as

A T. Brown *et al.* (2007)



B A. Raj *et al.* (2019)



C S. M. Goldup *et al.* (2020)

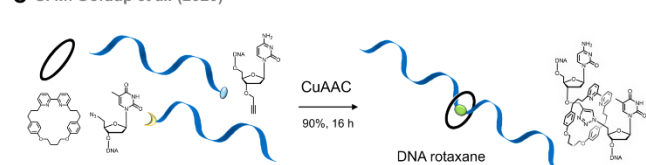


Figure 11. Creation of various nucleic acid threaded structures by CuAAC. (A) Catenane,⁸⁹ (B) multi-interlocked structure,⁹¹ and (C) rotaxane.⁹²

crosslinking. The reactions are remarkably accelerated on the templated DNA and RNA.^{89, 90} For example, the synthesis of a covalently closed DNA catenane was achieved using two ODNs modified with azide and alkyne groups at the 3' and 5' terminals, respectively (Figure 11A).⁸⁹ As an application, multi-interlocked structures were created via multiclick

reactions⁹¹ called clamp fluorescence in situ hybridization (clampFISH), which improved the fluorescence detection

N. C. Seeman *et al.* (2008)

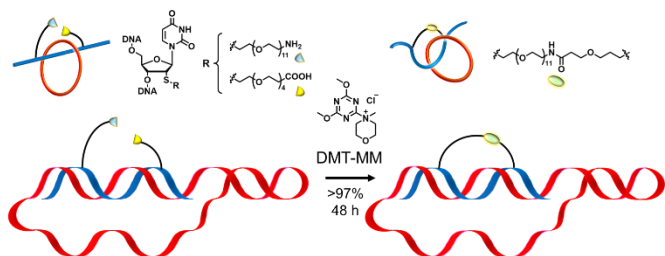


Figure 12. Formation of catenated DNA using DMT-MM.⁹⁵ Probe ODN was cyclized on a circular target DNA by amidation with DMT-MM.

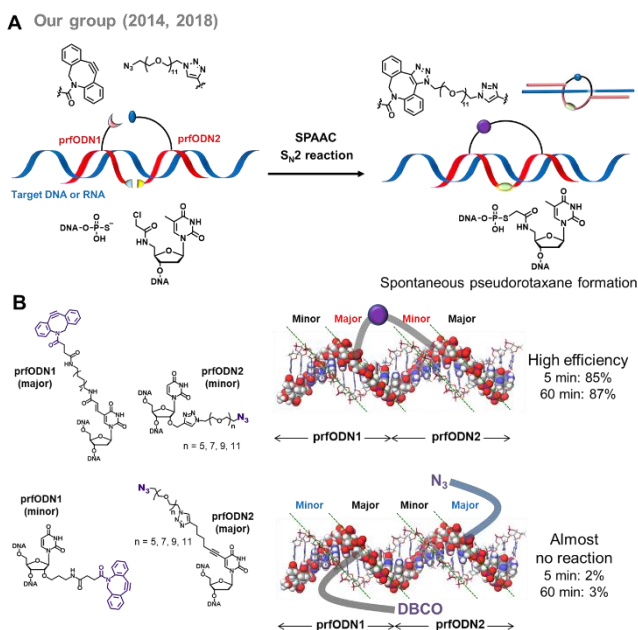


Figure 13. Spontaneous pseudorotaxane formation with prfODNs. (A) Formation scheme. The SPAAC and S_N2 reactions were accelerated by hybridization with target DNA or RNA.⁹⁶ (B) Optimization of pseudorotaxane formation.⁹⁷ The major–minor combination showed efficient pseudorotaxane formation. In contrast, almost no reaction occurred using the minor–major combination. The yields indicate the pseudorotaxane formation with the RNA target.

method of nucleic acids. ClampFISH achieved high specificity and gain (>400-fold) signal amplification (Figure 11B). The high reaction efficiency of CuAAC enabled the creation of this multi-interlocked structure and the amplification of the fluorescent RNA signals. More recently, an active metal template synthesis approach was used for synthesizing DNA rotaxanes with precise control on the position of the macrocycle (Figure 11C).⁹² The small-sized macrocycle cannot move and separate from the DNA strand after CuAAC because the nucleotide adjacent to the macrocycle is sufficiently large to act as a stopper of rotaxane. Although this method is not a

hybridization-specific chemical reaction, it is useful for creating DNA-rotaxane in high yields. It is expected that this type of rotaxane will be used for developing bioactivity-controllable oligonucleotides using cleavable macrocycles that can be removed in response to external or biological stimuli.

Amidation with DMT-MM,^{93, 94} which is a condensing agent that can be used in water, is also a useful reaction to create interlocked nucleic acid structures. The ODN modified with amine and carboxylic acid via linkers formed a duplex with circular target DNAs, creating catenanes via DMT-MM amidation (Figure 12).⁹⁵ This amide linkage across a full turn of DNA helix was an alternative method for chemical ligation and generated a double-tailed catenane. Using this type of catenane formation, DNA labeling was achieved without covalent linkages to the target nucleic acids in high yields.

To expand the unique properties of the threaded and interlocked structures into life sciences and nanotechnology, a spontaneous rotaxane formation method without external stimuli, such as chemical reagents or photoirradiation, would be ideal. Based on the previously mentioned studies, we designed automatic pseudorotaxane-forming oligo DNAs (prfODNs) (Figure 13A).⁹⁶ A pair of reactive prfODNs (prfODN1 and prfODN2) contained the reactive moieties. PrfODN1 contained a dibenzocyclooctyne (DBCO) group at the internal position and a phosphorothioate group at the 3' terminal, whereas prfODN2 contained an azide group at the internal position and a chloroacetoamide group at the 5' terminal. When these prfODNs were hybridized with the DNA or RNA target at the same time and target positions, an S_N2 -type chemical ligation reaction proceeded between the phosphorothioate and chloroacetoamide groups. Strain-promoted azide–alkyne cycloaddition (SPAAC) between the DBCO and azide groups then proceeded across a helical turn to provide the pseudorotaxane structure.

The designed prfODNs successfully formed the pseudorotaxane structure with DNA and RNA targets. Additionally, after the systematic optimization of the prfODNs, we found that the modification positions of the DBCO and azide groups are important for an efficient reaction (Figure 13B).⁹⁷ When prfODN1 contained the DBCO group at the major groove side and prfODN1 contained the azide group at the minor groove side (major–minor combination), the most efficient SPAAC reaction proceeded regardless of the linker length. The yield for the RNA target reached 85% in 5 min because the reactive groups react with each other via the shortest distance. Conversely, in the minor–major combination, almost no reaction occurred because the reactive groups could not approach each other. The optimized prfODNs with the major–minor combination could form the pseudorotaxane structure with a small ring size and the structure significantly increased the kinetic stability. Furthermore, the catenane structure was successfully formed with the optimized prfODNs and cyclized target DNA to provide conclusive evidence for forming a threaded structure. This type of rotaxane-like structure would enable the noncovalent labeling of RNAs and become a new tool to control gene expression.

In the above investigation, we found that the chemically cyclized ODN (cyODN) with a double-tail formed a pseudorotaxane structure with the target via a slippage process (Figure 14).⁹⁸ Interestingly, the efficiency of the pseudorotaxane formation increased with increasing temperature, reaching a peak at 50 °C. Further experiments indicated that the formation efficiency significantly depended on the ring size, target length, and mismatched position of the target in addition to the temperature. The best cyODN formed pseudorotaxane with short target DNA within 2 h, with a yield of 95%. This slippage formation can be divided into two steps: pre-equilibrium and threading steps (Figure 14). The formation of the intermediate in the pre-equilibrium step would guide the threading by through the efficient approach of the ring part to the end of the target. This efficient slippage mechanism resembles hybridization-specific chemical reactions in that it is accelerated by the proximity effect. Using the properties of the pseudorotaxane formation and dissociation, thermoreversible pseudorotaxane formation has been demonstrated. If the photoresponse moiety, such as azobenzene derivatives,⁹⁹ is incorporated into the cyODN, the photoreversible pseudorotaxane formation could be possible, which will be a useful tool for dynamic DNA/RNA nanotechnology.

4. Conclusions

In this review, we have summarized hybridization-specific chemical reactions for creating the interstrand crosslinking and threaded structures of nucleic acids. The reactions are accelerated by the proximity effect in the hybridization-specific reaction fields, achieving efficient and selective creations. To expand structural diversity, the creation of reaction fields and the discovery of useful reactions are important. Regarding the crosslinking reaction, we introduced Michael-like reactions by vinyl chemistry, imine derivative formations, CuAACs, and photocycloadditions. Each reaction provides different structures and functions with different efficiencies and yields; hence, we should select an appropriate reaction according to the purpose. Creating simple or unique structures with high efficiency and yield will provide more opportunities to develop functional nucleic acids. Regarding the functions of the crosslinking structure, we introduced anti-miRNA, decoy, and siRNA with high thermal and enzymatic stability obtained by the crosslinking structures. The reversible crosslinking is also useful for creating reversible photoresponsive gels and DNA origami objects in DNA nanotechnology. The high efficiency and yield of photoreversible reactions at high wavelengths make it a more powerful tool for creating materials with useful functions. Because our flipped-out crosslinking is a novel structure, we will explore its novel biological functions and nanotechnology applications. Regarding the functions of threaded structures, topological labels are powerful tools because covalent linkage to the target nucleic acids is not required and multiple labels are possible. However, there are still few effective cases of intracellular use. The recent progress in the creation of threaded structures is expected to develop new intracellular functional nucleic acids with

threaded structures. The caged oligonucleotides as well as

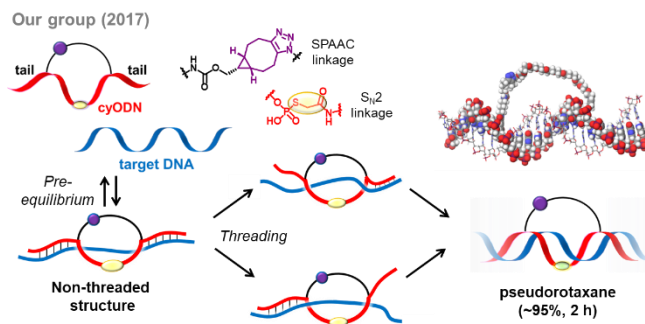


Figure 14. Pseudorotaxane formation with cyODNs via a slippage process.⁹⁸

catenane labeling of circular RNAs and functionalized mRNAs with the noncovalent threaded structures will be powerful tools in oligonucleotide therapeutics and chemical biology. A further reaction development and the discovery of their applications are desired to expand the research field of interstrand crosslinking and threaded structures.

Conflicts of interest

There are no conflicts to declare.

Acknowledgments

We acknowledge the financial supports from a Grant-in-Aid for Scientific Research on Innovative Areas "Middle Molecular Strategy" (No. JP15H05838 to F.N.), "Frontier Research on Chemical Communications" (No. JP20H04762 to K.O.), Scientific Research (B) (No. JP19H02845 to K.O.), (No. JP20H02855 to F.N.), and Challenging Exploratory Research (No. JP21K19323 to K.O.) from the Japan Society for the Promotion of Science, Japan Science and Technology Agency FOREST program (No. JPMJFR2002 to K.O.), Konica Minolta Award in Synthetic Organic Chemistry, Japan (K.O.), the TOBE MAKI Scholarship Foundation (K.O.), and the research program of "Dynamic Alliance for Open Innovation Bridging Human, Environment and Materials."

References

1. K. Gorska and N. Winssinger, *Angew. Chem. Int. Ed.*, 2013, **52**, 6820-6843.
2. C. Percivalle, J. F. Bartolo and S. Ladame, *Org. Biomol. Chem.*, 2013, **11**, 16-26.
3. R. K. O'Reilly, A. J. Turberfield and T. R. Wilks, *Acc. Chem. Res.*, 2017, **50**, 2496-2509.
4. M. Di Pisa and O. Seitz, *ChemMedChem*, 2017, **12**, 872-882.
5. B. Koo, H. Yoo, H. J. Choi, M. Kim, C. Kim and K. T. Kim, *Molecules*, 2021, **26**, 556.
6. S. Imoto, T. Hori, S. Hagihara, Y. Taniguchi, S. Sasaki and F. Nagatsugi, *Bioorg. Med. Chem. Lett.*, 2010, **20**, 6121-6124.

7. S. Hagihara, S. Kusano, W. C. Lin, X. G. Chao, T. Hori, S. Imoto and F. Nagatsugi, *Bioorg. Med. Chem. Lett.*, 2012, **22**, 3870-3872.
8. S. Hagihara, W. C. Lin, S. Kusano, X. G. Chao, T. Hori, S. Imoto and F. Nagatsugi, *ChemBioChem*, 2013, **14**, 1427-1429.
9. F. Nagatsugi and S. Imoto, *Org. Biomol. Chem.*, 2011, **9**, 2579-2585.
10. K. Hattori, T. Hirohama, S. Imoto, S. Kusano and F. Nagatsugi, *Chem. Commun.*, 2009, 6463-6465.
11. Y. Taniguchi, Y. Kurose, T. Nishioka, F. Nagatsugi and S. Sasaki, *Bioorg. Med. Chem.*, 2010, **18**, 2894-2901.
12. S. Kusano, T. Sakuraba, S. Hagihara and F. Nagatsugi, *Bioorg. Med. Chem. Lett.*, 2012, **22**, 6957-6961.
13. A. Nishimoto, D. Jitsuzaki, K. Onizuka, Y. Taniguchi, F. Nagatsugi and S. Sasaki, *Nucleic Acids Res.*, 2013, **41**, 6774-6781.
14. S. Kusano, T. Haruyama, S. Ishiyama, S. Hagihara and F. Nagatsugi, *Chem. Commun.*, 2014, **50**, 3951-3954.
15. S. Kusano, S. Ishiyama, S. L. Lam, T. Mashima, M. Katahira, K. Miyamoto, M. Aida and F. Nagatsugi, *Nucleic Acids Res.*, 2015, **43**, 7717-7730.
16. K. Kikuta, H. Piao, J. Brazier, Y. Taniguchi, K. Onizuka, F. Nagatsugi and S. Sasaki, *Bioorg. Med. Chem. Lett.*, 2015, **25**, 3307-3310.
17. T. Akisawa, Y. Ishizawa and F. Nagatsugi, *Molecules*, 2015, **20**, 4708-4719.
18. T. Akisawa, K. Yamada and F. Nagatsugi, *Bioorg. Med. Chem. Lett.*, 2016, **26**, 5902-5906.
19. K. Yamada, Y. Abe, H. Murase, Y. Ida, S. Hagihara and F. Nagatsugi, *J. Org. Chem.*, 2018, **83**, 8851-8862.
20. N. Sato, G. Tsuji, Y. Sasaki, A. Usami, T. Moki, K. Onizuka, K. Yamada and F. Nagatsugi, *Chem. Commun.*, 2015, **51**, 14885-14888.
21. N. Sato, S. Takahashi, H. Tateishi-Karimata, M. E. Hazemi, T. Chikuni, K. Onizuka, N. Sugimoto and F. Nagatsugi, *Org. Biomol. Chem.*, 2018, **16**, 1436-1441.
22. K. Onizuka, A. Usami, Y. Yamaoki, T. Kobayashi, M. E. Hazemi, T. Chikuni, N. Sato, K. Sasaki, M. Katahira and F. Nagatsugi, *Nucleic Acids Res.*, 2018, **46**, 1059-1068.
23. M. E. Hazemi, K. Onizuka, T. Kobayashi, A. Usami, N. Sato and F. Nagatsugi, *Bioorg. Med. Chem.*, 2018, **26**, 3551-3558.
24. K. Onizuka, M. E. Hazemi, N. Sato, G. I. Tsuji, S. Ishikawa, M. Ozawa, K. Tanno, K. Yamada and F. Nagatsugi, *Nucleic Acids Res.*, 2019, **47**, 6578-6589.
25. K. Onizuka, E. Ganbold, Y. Ma, S. Sasaki, M. E. Hazemi, Y. Chen, N. Sato, M. Ozawa, K. Nagasawa and F. Nagatsugi, *Org. Biomol. Chem.*, 2021, **19**, 2891-2894.
26. F. Nagatsugi and K. Onizuka, *Chem. Lett.*, 2020, **49**, 771-780.
27. K. Onizuka, M. E. Hazemi, J. M. Thomas, L. R. Monteleone, K. Yamada, S. Imoto, P. A. Beal and F. Nagatsugi, *Bioorg. Med. Chem.*, 2017, **25**, 2191-2199.
28. A. M. Abdelhady, Y. Hirano, K. Onizuka, H. Okamura, Y. Komatsu and F. Nagatsugi, *Bioorg. Med. Chem. Lett.*, 2021, **48**, 128257.
29. K. Ichikawa, N. Kojima, Y. Hirano, T. Takebayashi, K. Kowata and Y. Komatsu, *Chem. Commun.*, 2012, **48**, 2143-2145.
30. Y. Mie, Y. Hirano, K. Kowata, A. Nakamura, M. Yasunaga, Y. Nakajima and Y. Komatsu, *Mol. Ther. Nucleic Acids*, 2018, **10**, 64-74.
31. S. Dutta, G. Chowdhury and K. S. Gates, *J. Am. Chem. Soc.*, 2007, **129**, 1852-1853.
32. K. M. Johnson, N. E. Price, J. Wang, M. I. Fekry, S. Dutta, D. R. Seiner, Y. Wang and K. S. Gates, *J. Am. Chem. Soc.*, 2013, **135**, 1015-1025.
33. N. E. Price, K. M. Johnson, J. Wang, M. I. Fekry, Y. Wang and K. S. Gates, *J. Am. Chem. Soc.*, 2014, **136**, 3483-3490.
34. J. Gamboa Varela and K. S. Gates, *Angew. Chem. Int. Ed.*, 2015, **54**, 7666-7669.
35. M. I. Nejad, N. E. Price, T. Haldar, C. Lewis, Y. Wang and K. S. Gates, *ACS Chem. Biol.*, 2019, **14**, 1481-1489.
36. A. H. Kellum, D. Y. Qiu, M. W. Voehler, W. Martin, K. S. Gates and M. P. Stone, *Biochemistry*, 2021, **60**, 41-52.
37. A. H. El-Sagheer and T. Brown, *Chem. Soc. Rev.*, 2010, **39**, 1388-1405.
38. N. Z. Fantoni, A. H. El-Sagheer and T. Brown, *Chem. Rev.*, 2021, **121**, 7122-7154.
39. J. Gierlich, G. A. Burley, P. M. E. Gramlich, D. M. Hammond and T. Carell, *Org. Lett.*, 2006, **8**, 3639-3642.
40. H. Peacock, O. Maydanovych and P. A. Beal, *Org. Lett.*, 2010, **12**, 1044-1047.
41. K. Onizuka, A. Shibata, Y. Taniguchi and S. Sasaki, *Chem. Commun.*, 2011, **47**, 5004-5006.
42. K. Onizuka, J. G. Harrison, A. A. Ball-Jones, J. M. Ibarra-Soza, Y. Zheng, D. Ly, W. Lam, S. Mac, D. J. Tantillo and P. A. Beal, *J. Am. Chem. Soc.*, 2013, **135**, 17069-17077.
43. P. Kocalka, A. H. El-Sagheer and T. Brown, *ChemBioChem*, 2008, **9**, 1280-1285.
44. M. Nakane, S. Ichikawa and A. Matsuda, *J. Org. Chem.*, 2008, **73**, 1842-1851.
45. Y. Yoshimura and K. Fujimoto, *Org. Lett.*, 2008, **10**, 3227-3230.
46. T. Sakamoto, Y. Tanaka and K. Fujimoto, *Org. Lett.*, 2015, **17**, 936-939.
47. K. Fujimoto, S. Sasago, J. Mihara and S. Nakamura, *Org. Lett.*, 2018, **20**, 2802-2805.
48. A. Shigeno, T. Sakamoto, Y. Yoshimura and K. Fujimoto, *Org. Biomol. Chem.*, 2012, **10**, 7820-7825.
49. K. Fujimoto, H. Yang-Chun and S. Nakamura, – *Chem. Asian J.*, 2019, **14**, 1912-1916.
50. K. Fujimoto, K. Konishi-Hiratsuka, T. Sakamoto and Y. Yoshimura, *Chem. Commun.*, 2010, **46**, 7545-7547.
51. S. Nakamura, K. Ishino and K. Fujimoto, *ChemBioChem*, 2020, **21**, 3067-3070.
52. K. Fujimoto, K. Toyosato, S. Nakamura and T. Sakamoto, *Bioorg. Med. Chem. Lett.*, 2016, **26**, 5312-5314.
53. K. Fujimoto, M. Hashimoto, N. Watanabe and S. Nakamura, *Bioorg. Med. Chem. Lett.*, 2019, **29**, 2173-2177.
54. K. Fujimoto and N. Watanabe, *ChemistrySelect*, 2020, **5**, 14670-14676.
55. D. Kandatsu, K. Cervantes-Salguero, I. Kawamata, S. Hamada, S.-i. M. Nomura, K. Fujimoto and S. Murata, *ChemBioChem*, 2016, **17**, 1118-1121.
56. T. Gerling and H. Dietz, *Angew. Chem. Int. Ed.*, 2019, **58**, 2680-2684.
57. M. M. Haque, H. Sun, S. Liu, Y. Wang and X. Peng, *Angew. Chem. Int. Ed.*, 2014, **53**, 7001-7005.
58. H. Kashida, T. Doi, T. Sakakibara, T. Hayashi and H. Asanuma, *J. Am. Chem. Soc.*, 2013, **135**, 7960-7966.
59. T. Doi, H. Kawai, K. Murayama, H. Kashida and H. Asanuma, *Chem. – Eur. J.*, 2016, **22**, 10533-10538.
60. K. Murayama, Y. Yamano and H. Asanuma, *J. Am. Chem. Soc.*, 2019, **141**, 9485-9489.

61. Y. Yamano, K. Murayama and H. Asanuma, *Chem. – Eur. J.*, 2021, **27**, 4599-4604.
62. Y. Kamiya, K. Iishiba, T. Doi, K. Tsuda, H. Kashida and H. Asanuma, *Biomater Sci.*, 2015, **3**, 1534-1538.
63. Y. Zhou, C. Li, J. Peng, L. Xie, L. Meng, Q. Li, J. Zhang, X. D. Li, X. Li, X. Huang and X. Li, *J. Am. Chem. Soc.*, 2018, **140**, 15859-15867.
64. A. M. Abdelhady, K. Onizuka, K. Ishida, S. Yajima, E. Mano and F. Nagatsugi, *J. Org. Chem.*, 2022, **87**, 2267-2276.
65. K. Onizuka, K. Ishida, E. Mano and F. Nagatsugi, *Org. Lett.*, 2019, **21**, 2833-2837.
66. H. J. Shine and D. C. Zhao, *J. Org. Chem.*, 1990, **55**, 4086-4089.
67. D. Wei and F. Liang, *Org. Lett.*, 2016, **18**, 5860-5863.
68. K. M. Chan, D. K. Kölmel, S. Wang and E. T. Kool, *Angew. Chem. Int. Ed.*, 2017, **56**, 6497-6501.
69. D. Ackermann, T. L. Schmidt, J. S. Hannam, C. S. Purohit, A. Heckel and M. Famulok, *Nat. Nanotechnol.*, 2010, **5**, 436-442.
70. T. L. Schmidt and A. Heckel, *Nano Lett.*, 2011, **11**, 1739-1742.
71. F. Lohmann, D. Ackermann and M. Famulok, *J. Am. Chem. Soc.*, 2012, **134**, 11884-11887.
72. Y. Sannohe and H. Sugiyama, *Bioorg. Med. Chem.*, 2012, **20**, 2030-2034.
73. X. Liu, C. H. Lu and I. Willner, *Acc. Chem. Res.*, 2014, **47**, 1673-1680.
74. Z. S. Wu, Z. Shen, K. Tram and Y. Li, *Nat. Commun.*, 2014, **5**, 4279.
75. J. T. Powell, B. O. Akhuetie-Oni, Z. Zhang and C. Lin, *Angew. Chem. Int. Ed.*, 2016, **55**, 11412-11416.
76. J. List, E. Falgenhauer, E. Kopperger, G. Pardatscher and F. C. Simmel, *Nat. Commun.*, 2016, **7**, 12414.
77. Q. Li, G. Wu, W. Wu and X. Liang, *ChemBioChem*, 2016, **17**, 1127-1131.
78. J. Valero, N. Pal, S. Dhakal, N. G. Walter and M. Famulok, *Nat. Nanotechnol.*, 2018, **13**, 496-503.
79. Z. Yu, M. Centola, J. Valero, M. Matthies, P. Šulc and M. Famulok, *J. Am. Chem. Soc.*, 2021, **143**, 13292-13298.
80. A. Rajendran, K. Krishnamurthy, S. Park, E. Nakata, Y. Kwon and T. Morii, *Chem. – Eur. J.*, 2022, **28**, e202200108.
81. M. Nilsson, H. Malmgren, M. Samiotaki, M. Kwiatkowski, B. P. Chowdhary and U. Landegren, *Science*, 1994, **265**, 2085-2088.
82. C. Escudé, T. Garestier and C. Hélène, *Proc. Natl. Acad. Sci. U. S. A.*, 1999, **96**, 10603-10607.
83. S. Wang and E. T. Kool, *Nucleic Acids Res.*, 1994, **22**, 2326-2333.
84. K. Ryan and E. T. Kool, *Chem. Biol.*, 1998, **5**, 59-67.
85. K. Fujimoto, S. Matsuda, N. Ogawa, M. Hayashi and I. Saito, *Tetrahedron Lett.*, 2000, **41**, 6451-6454.
86. K. Fujimoto, S. Matsuda, Y. Yoshimura, T. Ami and I. Saito, *Chem. Commun.*, 2007, 2968-2970.
87. M. Mukae, T. Ihara, M. Tabara and A. Jyo, *Org. Biomol. Chem.*, 2009, **7**, 1349-1354.
88. P. Arslan, A. Jyo and T. Ihara, *Org. Biomol. Chem.*, 2010, **8**, 4843-4848.
89. R. Kumar, A. El-Sagheer, J. Tumpene, P. Lincoln, L. M. Wilhelmsson and T. Brown, *J. Am. Chem. Soc.*, 2007, **129**, 6859-6864.
90. E. Paredes and S. R. Das, *ChemBioChem*, 2011, **12**, 125-131.
91. S. H. Rouhanifard, I. A. Mellis, M. Dunagin, S. Bayatpour, C. L. Jiang, I. Dardani, O. Symmons, B. Emert, E. Torre, A. Cote, A. Sullivan, J. A. Stamatoyannopoulos and A. Raj, *Nat. Biotechnol.*, 2019, **37**, 84-89.
92. A. Acevedo-Jake, A. T. Ball, M. Galli, M. Kukwikila, M. Denis, D. G. Singleton, A. Tavassoli and S. M. Goldup, *J. Am. Chem. Soc.*, 2020, **142**, 5985-5990.
93. M. Kunishima, C. Kawachi, J. Monta, K. Terao, F. Iwasaki and S. Tani, *Tetrahedron*, 1999, **55**, 13159-13170.
94. M. Kunishima, K. Yoshimura, H. Morigaki, R. Kawamata, K. Terao and S. Tani, *J. Am. Chem. Soc.*, 2001, **123**, 10760-10761.
95. Y. Liu, A. Kuzuya, R. Sha, J. Guillaume, R. Wang, J. W. Canary and N. C. Seeman, *J. Am. Chem. Soc.*, 2008, **130**, 10882-10883.
96. K. Onizuka, F. Nagatsugi, Y. Ito and H. Abe, *J. Am. Chem. Soc.*, 2014, **136**, 7201-7204.
97. K. Onizuka, T. Miyashita, T. Chikuni, M. Ozawa, H. Abe and F. Nagatsugi, *Nucleic Acids Res.*, 2018, **46**, 8710-8719.
98. K. Onizuka, T. Chikuni, T. Amemiya, T. Miyashita, K. Onizuka, H. Abe and F. Nagatsugi, *Nucleic Acids Res.*, 2017, **45**, 5036-5047.
99. Y. Kamiya and H. Asanuma, *Acc. Chem. Res.*, 2014, **47**, 1663-1672.